

8-1968

Crossed Field Trochoidal Trajectory Devices for Investigating the Reflection of Slow Electrons from Metallic Surfaces

Stan Lemaster
Western Kentucky University

Follow this and additional works at: <https://digitalcommons.wku.edu/theses>



Part of the [Engineering Physics Commons](#)

Recommended Citation

Lemaster, Stan, "Crossed Field Trochoidal Trajectory Devices for Investigating the Reflection of Slow Electrons from Metallic Surfaces" (1968). *Masters Theses & Specialist Projects*. Paper 2527.
<https://digitalcommons.wku.edu/theses/2527>

This Thesis is brought to you for free and open access by TopSCHOLAR®. It has been accepted for inclusion in Masters Theses & Specialist Projects by an authorized administrator of TopSCHOLAR®. For more information, please contact topscholar@wku.edu.

Lemaster,

Stan W.

1968

CROSSED FIELD TROCHOIDAL TRAJECTORY DEVICES
FOR INVESTIGATING THE REFLECTION
OF SLOW ELECTRONS FROM
METALLIC SURFACES

BY
STAN W. LEMASTER

A THESIS
SUBMITTED IN PARTIAL FULFILLMENT
OF THE REQUIREMENTS FOR THE DEGREE OF
MASTER OF SCIENCE IN ENGINEERING PHYSICS

WESTERN KENTUCKY UNIVERSITY

AUGUST 1968

WEST. KY. UNIV. LIB.

CROSSED FIELD TROCHOIDAL TRAJECTORY DEVICES
FOR INVESTIGATING THE REFLECTION
OF SLOW ELECTRONS FROM
METALLIC SURFACES

F. M. Carter

Thesis Advisor

W. F. Aij
William G. Beckman

John Don Munton

Dean of Graduate School

ACKNOWLEDGMENTS

The author wishes to acknowledge the kind assistance and helpful guidance of Floyd M. Carter who directed this research.

The work of Dr. M. W. Russell, Dr. George C. Moore, Dr. W. W. Hunt, J. D. Marshall, J. D. Burd, H. Gailbrath, and K. E. Garrison who contributed information included in this paper, was greatly appreciated.

TABLE OF CONTENTS

	Page
ACKNOWLEDGEMENTS.....	ii
LIST OF TABLES.....	iv
LIST OF FIGURES.....	v
 Chapter	
I. INTRODUCTION.....	1
Background and objectives.....	1
Crossed field approach.....	1
 II. DESIGN CONSIDERATIONS AND CONSTRUCTION FEATURES.....	 4
Choice of material.....	4
Selection of envelope.....	4
Processing.....	4
Types of electron guns chosen.....	7
Helmholtz coils.....	7
Photographs of devices.....	13
 III. EXPERIMENTAL RESULTS.....	 17
Magnetic shielding problems.....	17
Calculation of reflection coefficient.....	19
Pencil beam results.....	24
Sheet beam results.....	29
Zero electric field results.....	34
 IV. ANALYSIS OF RESULTS.....	 37
Comparison of the various trochoidal devices.....	41
Summary.....	42
Recommendations for future work.....	43
 LIST OF REFERENCES.....	 44
BIOGRAPHICAL SKETCH.....	45

LIST OF TABLES

Table	Page
1. Data taken from pencil beam device.....	25
2. Data taken from zero electric field device..	36

LIST OF FIGURES

Figure	Page
1. Previously published data for tungsten (1,1,0).....	3
2. Prototype model.....	5
3. Concept of the first pencil beam device.....	6
4. Sketch and photograph of Helmholtz coils.....	8
5. Schematic diagram of electrodes and equipotential lines.....	10
6. Initial pencil beam device.....	13
7. Final pencil beam device.....	14
8. Sheet beam device.....	15
9. Zero electric field device.....	16
10. Diagram of apparatus and curves showing method used to find reflection coefficient.....	21
11. Data taken during operation of initial pencil beam device.....	22
12. Investigation of magnetic shielding materials.....	23
13. Circuit used to evaluate final pencil beam device.....	24
14. Final pencil beam device collector current versus magnetic field for 2 ev electrons.....	26
15. Final pencil beam device collector current versus magnetic field for 4 ev electrons.....	27
16. Data taken during operation of pencil beam device for 5 ev electrons.....	28
17. Circuit used to evaluate sheet beam device.....	29
18. Sheet beam device cup & electrode current versus magnetic field for 5 ev electrons.....	30

Figure	Page
19. Sheet beam device cup & electrode current versus magnetic field for 10 ev electrons.....	31
20. Sheet beam device cup current versus magnetic field for 91 volt top electrode potential.....	32
21. Data taken on sheet beam device to determine reflection coefficient.....	33
22. Circuit used to evaluate zero electric field device...	34
23. Cup & top electrode current vs. magnetic field for zero electric field device.....	35
24. Sheet beam device with ionized mercury gas inside.....	39
25. Ionization patterns observed inside the sheet beam device during operation with mercury gas inside.....	40
26. Bottom electrode for initial pencil beam device.....	44

CHAPTER I

INTRODUCTION

The objective of this study was to build preliminary devices which could be used to measure electron reflection coefficient values using crossed electric and magnetic fields. The technique for using crossed fields to measure reflection coefficients was developed at Air Force Cambridge Research Laboratories. The reflection coefficient is the ratio of the number of electrons in a reflected beam to the number of electrons in an incident beam striking a surface.

The work described herein was a part of a project authorized by AFCRL under contract AF19 (628)-5940; Project 8605 (with Western Kentucky University being the contractor) which was entitled "An Investigation of the Reflection of Slow Electrons from Surfaces."¹ Earlier researchers working on the problem of measuring reflection coefficients generally had used large electron optical systems with target collection chambers.² Since their findings varied so considerably (Figure 1) it was decided to try a new approach. The results shown are curves describing the values obtained when electrons bombarded tungsten metal with energies ranging between .1 and 3.5 electron volts.

Basically the devices discussed within this paper consist of two parallel electrodes to provide a uniform electric field and an electron gun to inject electrons with known energy levels into the

field perpendicular to the electrodes. Each device utilized a Faraday cup to collect the electrons after the application of an external uniform magnetic field which bent the originally straight electron beam into a trochoidal path.

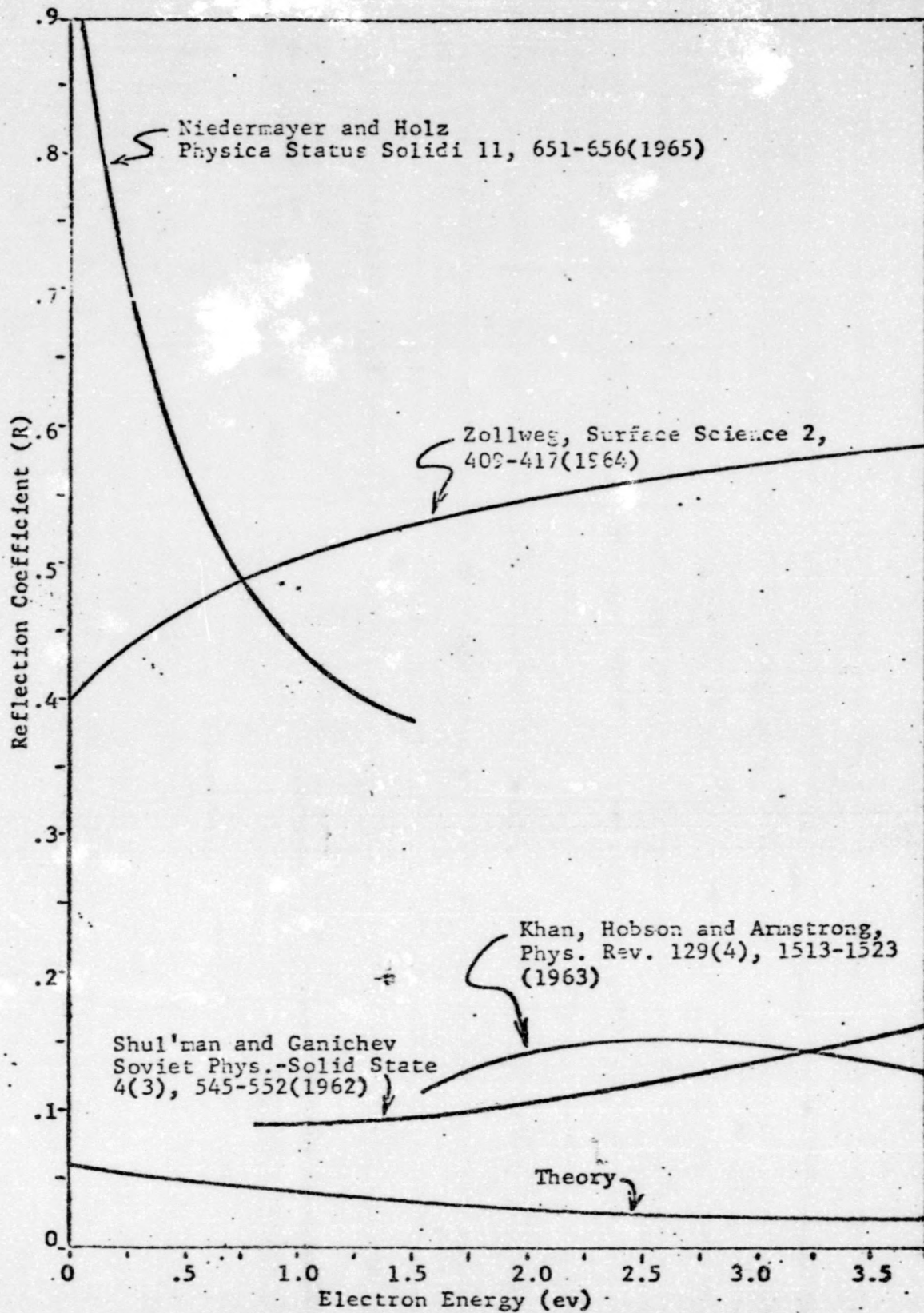


Figure 1. Previously published data for tungsten (1,1,0)

CHAPTER II

DESIGN CONSIDERATIONS AND CONSTRUCTION FEATURES

Because 302 stainless steel was available, inexpensive and easily formed into intricate shapes, it was chosen as the material to be used for the prototype electric field electrodes. A design was formulated which was simpler and smaller than known previous ones. It was tailored to use as many parts as possible from a conventional T-12 receiving tube (Figure 2) to facilitate exhaust and processing of the electron source. The initial device was planned to cause a 5 electron-volt electron to be injected at a right angle into a 10 gauss magnetic field. Calculations of the various distances between the cusps of the trochoidal path that the electron would follow dictated 1.5-2.0 centimeters between the beginning and end of the trajectory. A concept of the prototype is shown in Figure 3. The devices were assembled using the standard receiving tube practices and techniques of pre-firing the metal parts and assembling under "clean" conditions and then exhausting on an exhaust bench.³ After exhaust the device was operated for sixteen hours to stabilize the cathode emission inside the electron source. Stabilization is a necessary requirement for tubes. The devices included a getter which lowered the internal pressure to a level which permitted high vacuum

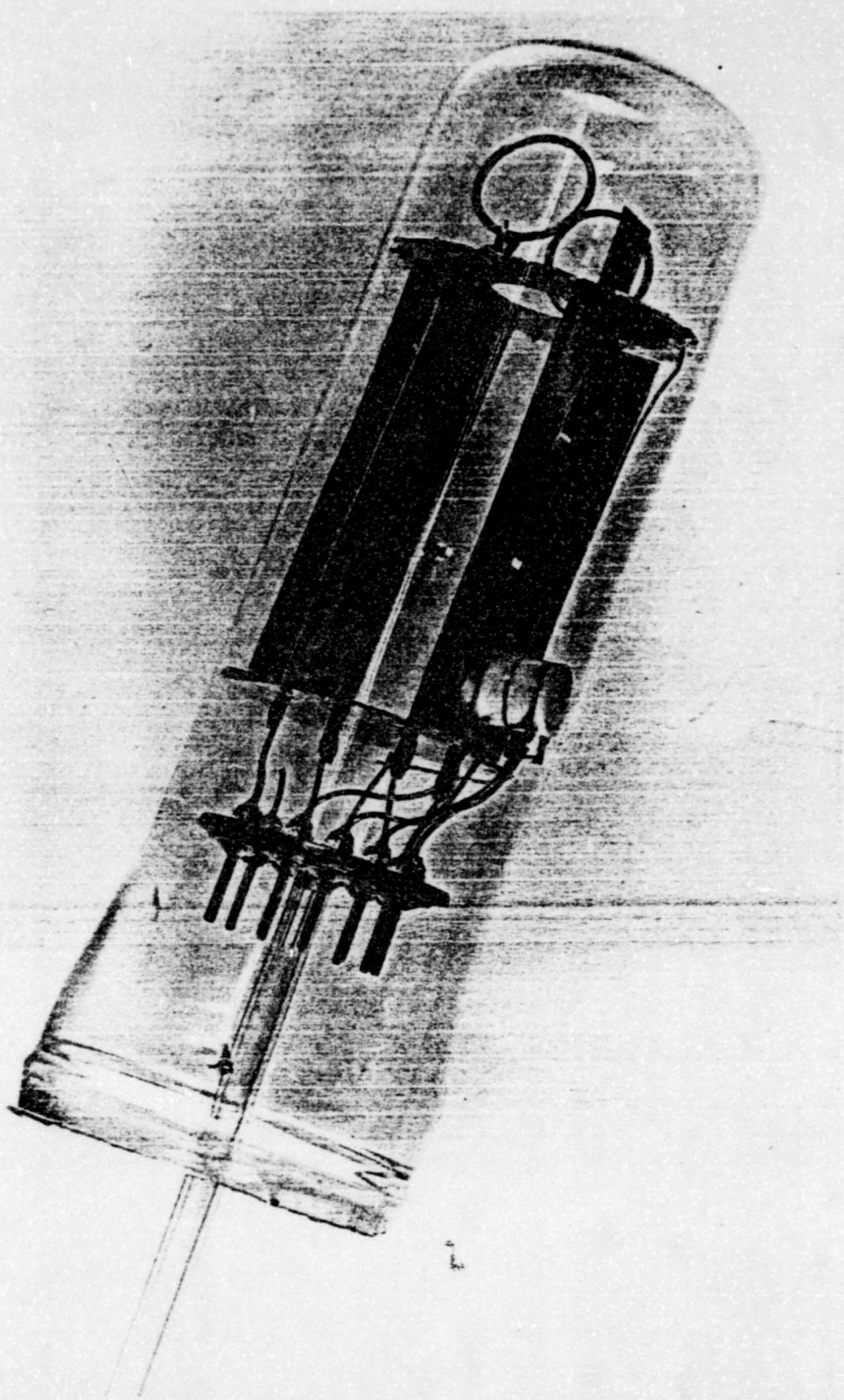


Figure 2. Prototype model.

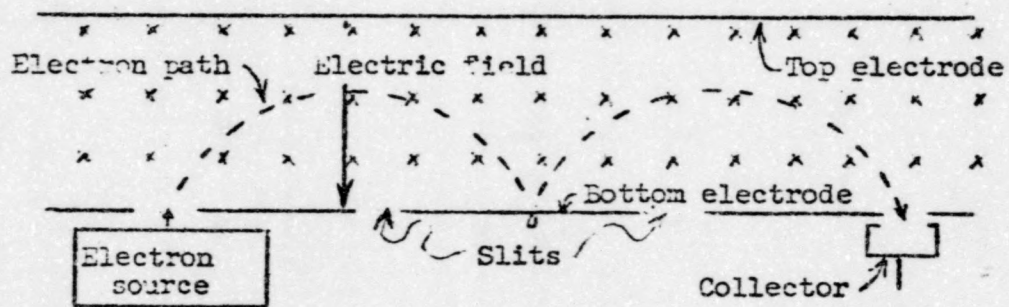


Figure 3. Concept of the first pencil beam device.

operation with a unipotential oxide cathode electron source. The electron guns used to inject electrons into the crossed electric and magnetic fields were of four general types: (1) Pierce, (2) modified Pierce, (3) sheet beam and (4) planar.

Helmholtz coils (Figure 4) were constructed to provide a uniform magnetic field for small test devices located at the center. Using the basic equation for the magnetic field intensity at the center of a coil:

$$H = \frac{32}{\sqrt{125}} \frac{NI}{r}$$

where N = number of turns on each coil

and I = current through coils in absolute amperes (abamperes)

and r = mean radius of coils in centimeters

and $B = \mu H$

where μ = permeability

now when $\mu = 1$, then $H = B$.

Once B was determined then $B(\text{effective}) = B(\text{calculated}) - B(\text{earth})$, providing that the coil is properly oriented. After $B(\text{effective})$ was determined then the radius was determined from the relationship:⁵

$$\frac{e}{m} = \frac{2V}{B^2 r^2}$$

where V = potential difference

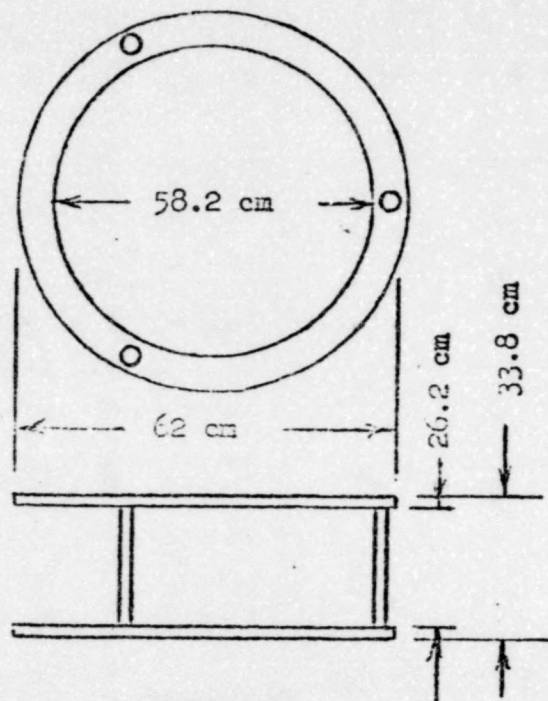


Figure 4. Sketch and photograph of Helmholtz coils.

and e = charge of electron

and m = mass of electron

The above equation can be transposed to provide expressions for B and r :

$$B = \sqrt{\frac{2V}{r^2 (e/m)}} \quad \text{and} \quad r = \sqrt{\frac{2V}{B^2 (e/m)}}$$

The coils were designed so that a magnetic field of 10 gauss would cause an electron entering it perpendicularly to be bent into a circle having a radius of 1 centimeter if its energy were 10 ev.

To determine the electrode cross-section which would exhibit the lowest amount of "fringing" of the electric field a plain electrolytic tank was designed and constructed to map electrostatic fields which would be formed by various electrode shapings (Figure 5). Measurements in the electrolytic tank using a probe and finding equipotential lines demonstrated that the electrostatic field between the outer edges of the electrodes could be made more uniform if the edges of the electrodes were bent inward at an angle of 25 degrees. This feature can be seen in Figure 24. The small contact area between the electrolyte and probe necessitated a high impedance detector. Analytical methods of checking the electrolytic tank measurements indicated that the error was less than 0.3%.⁶ Many other edge shapes were investigated but none had a greater electric field homogeneity than the one shown in Figure 5.

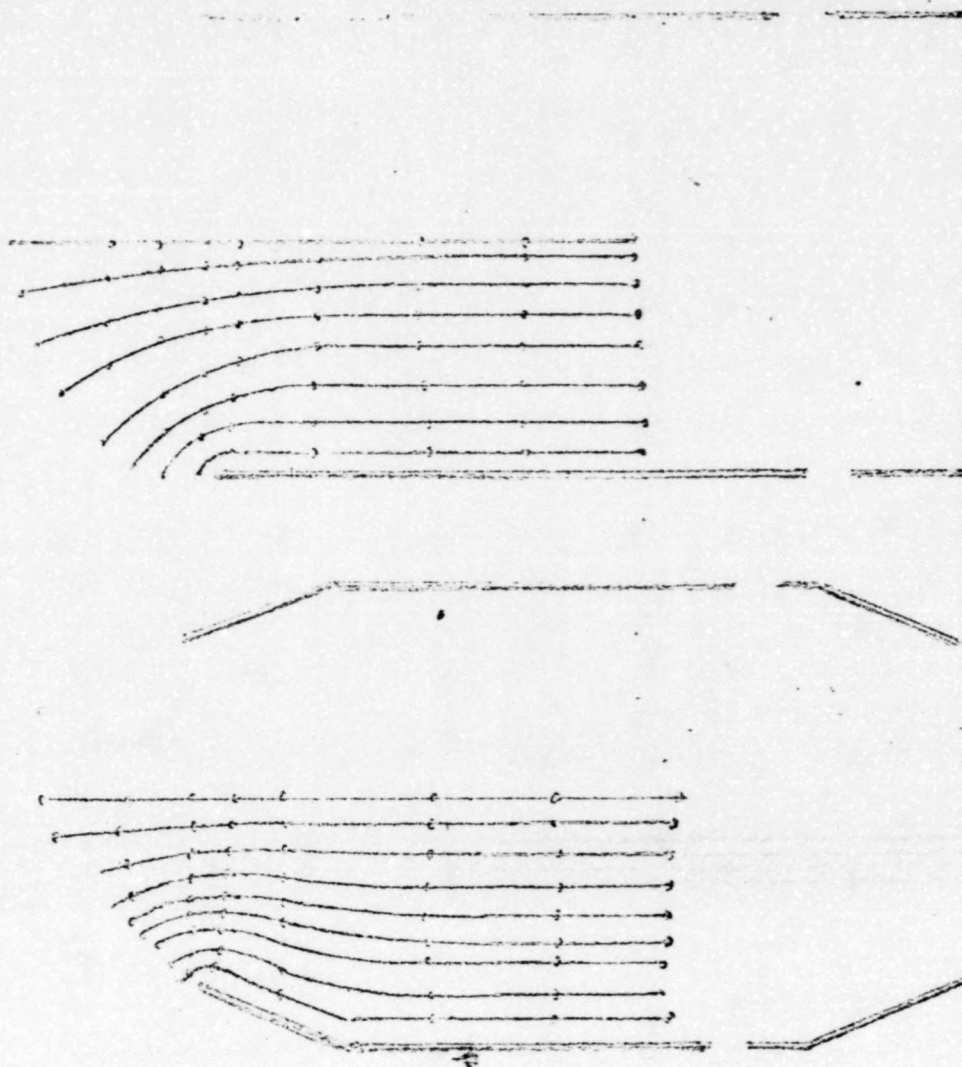


Figure 5. Schematic diagram of electrodes and equipotential lines.

Slits were placed in the bottom electrode to help determine the dimensions between the cusps of the trochoidal electron beam path (Figures 2 and 3). It can be noted that if the electron path can be adjusted so that it touches down in a slit with a suitable collector underneath then there would be a decrease in the bottom electrode current.

The collector (Faraday cup) was placed under a slot and shaped into a box for the purpose of trapping entering electrons.

The spacers used to position the electrodes in the devices were T-12 micas with magnesium oxide sprayed on their surfaces to retard leakage currents. Holes were punched in the micas in the area of the electric field to reduce the likelihood of the insulator acquiring an electrical charge.

The initial pencil beam device (Figure 6) was designed to cause the electron to go through two bounces before being intercepted by the collector. It will be noted that there is no magnetic shielding around the Pierce electron gun.

The final pencil beam device (Figure 7) was essentially the same as the initial pencil beam device with the exceptions of the magnetic shielding surrounding the electron gun and an Einzel lens in the electron gun.

The sheet beam device (Figure 8) was designed to cause the electron to go through a single bounce before being intercepted by the collector. It incorporated a sheet beam electron source. The emitting surface in the electron source was moved closer to the bottom electrode to minimize the bending of the electron beam within the gun by the applied magnetic field.

The zero electric field device (Figure 9) was designed to use magnetic deflection only. The device utilized a planar gun which moved the emitting surface in the electron source even closer to the bottom electrode than the sheet beam design. The collector had a gold plated tungsten mesh in front of it to trap any electron reaching its surface. The top and bottom electrodes were made from a single piece to insure a zero electric field between them.

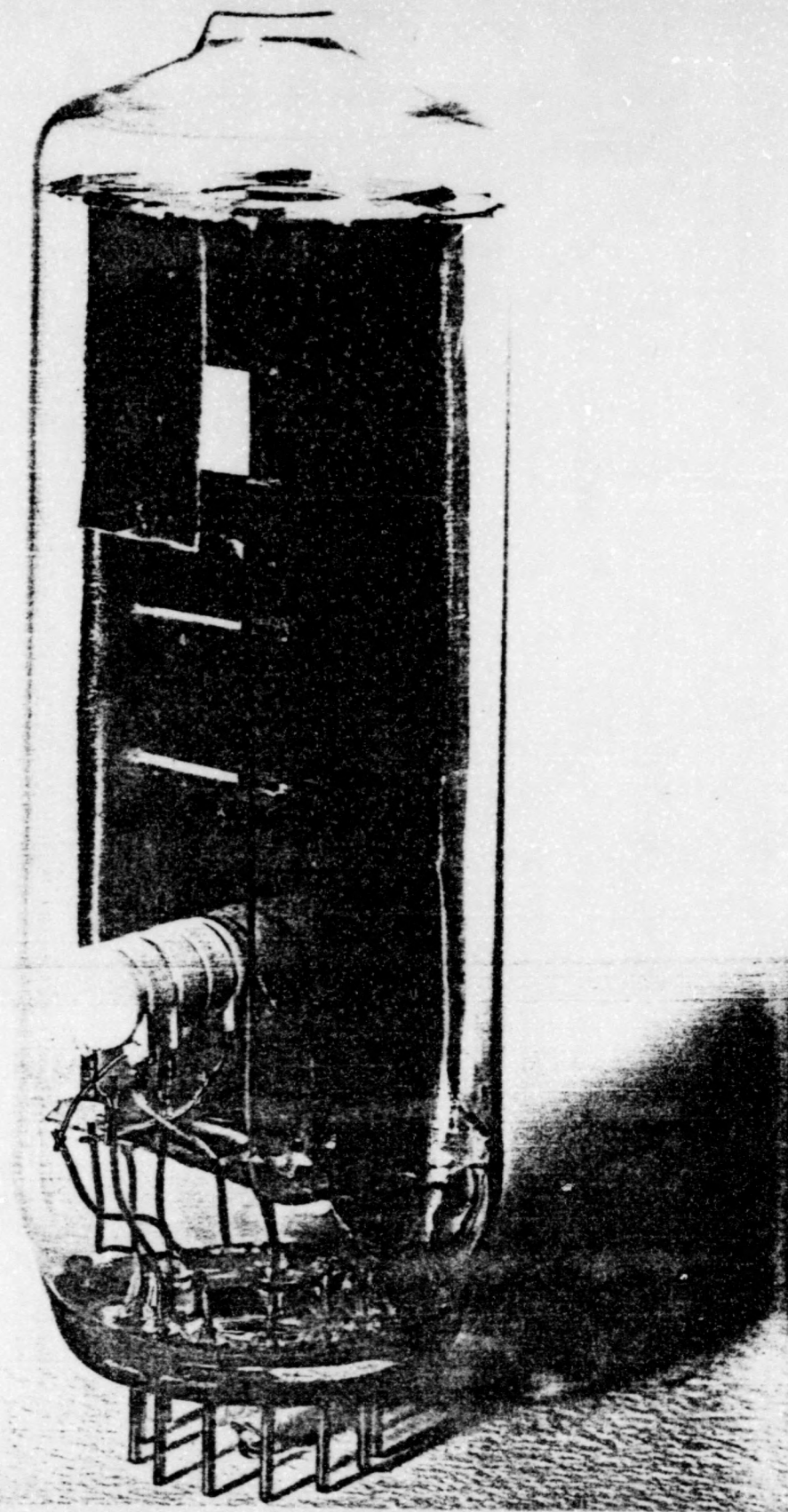


Figure 6. Initial pencil beam device.

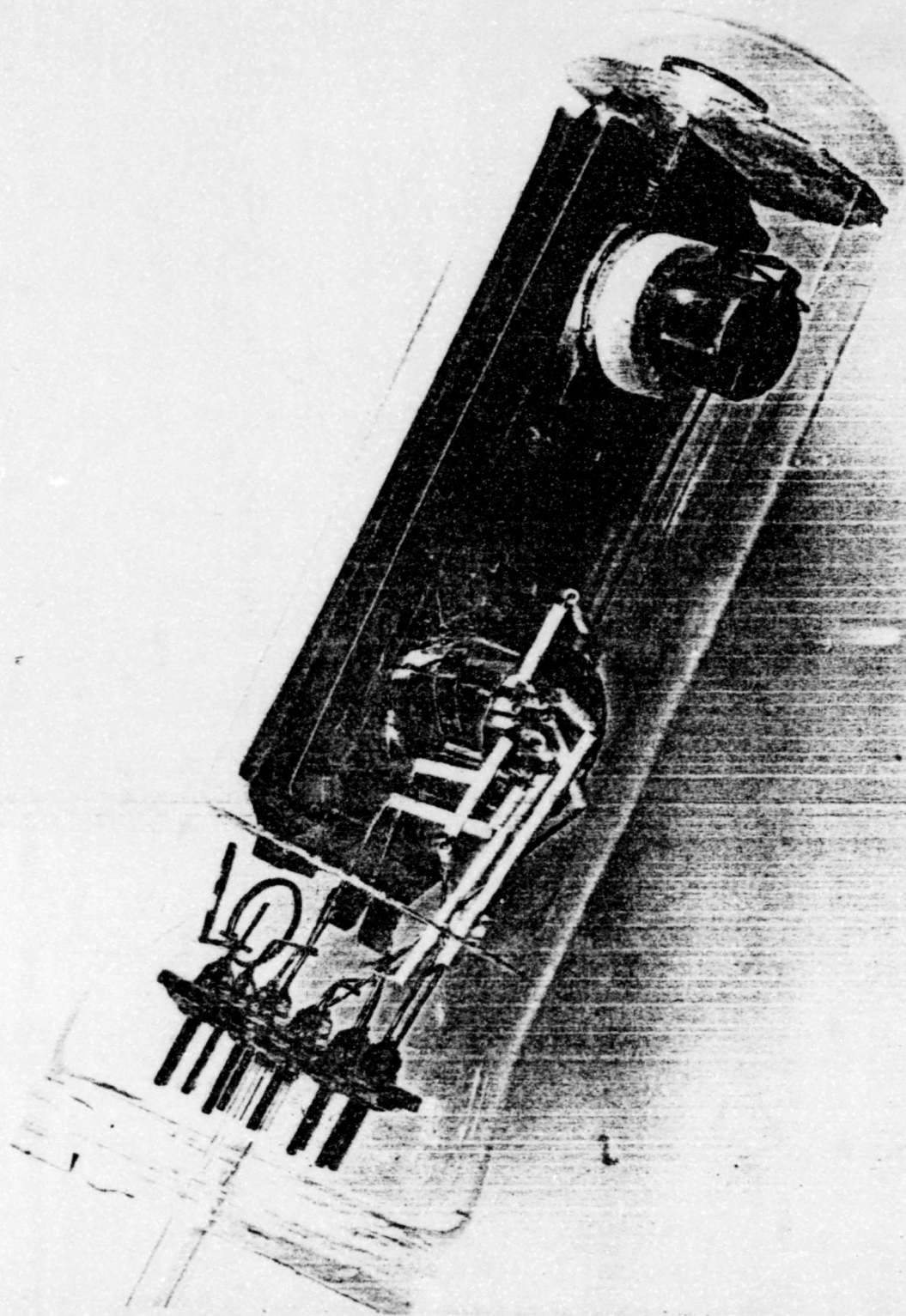


Figure 7. Final pencil beam device.

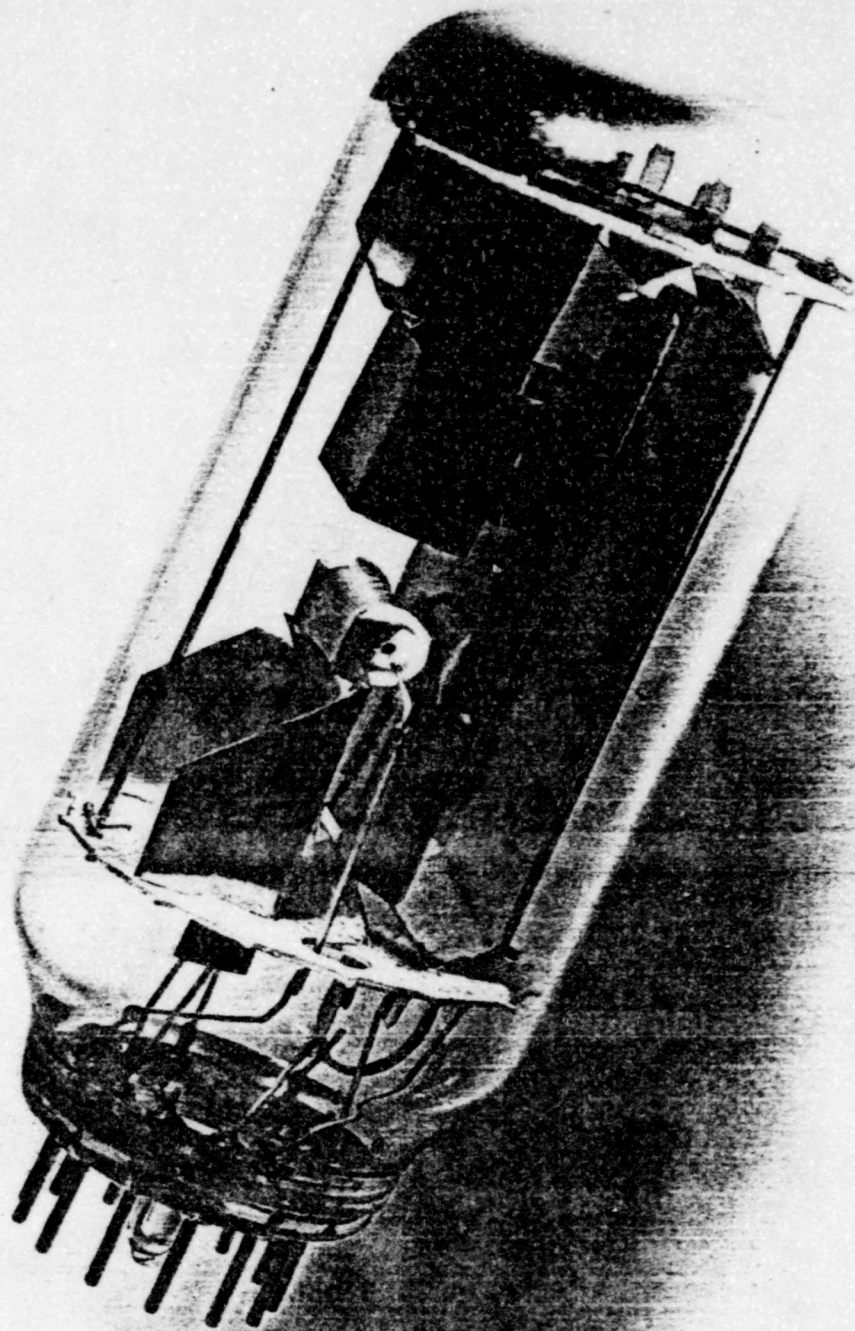


Figure 8. Sheet beam device.

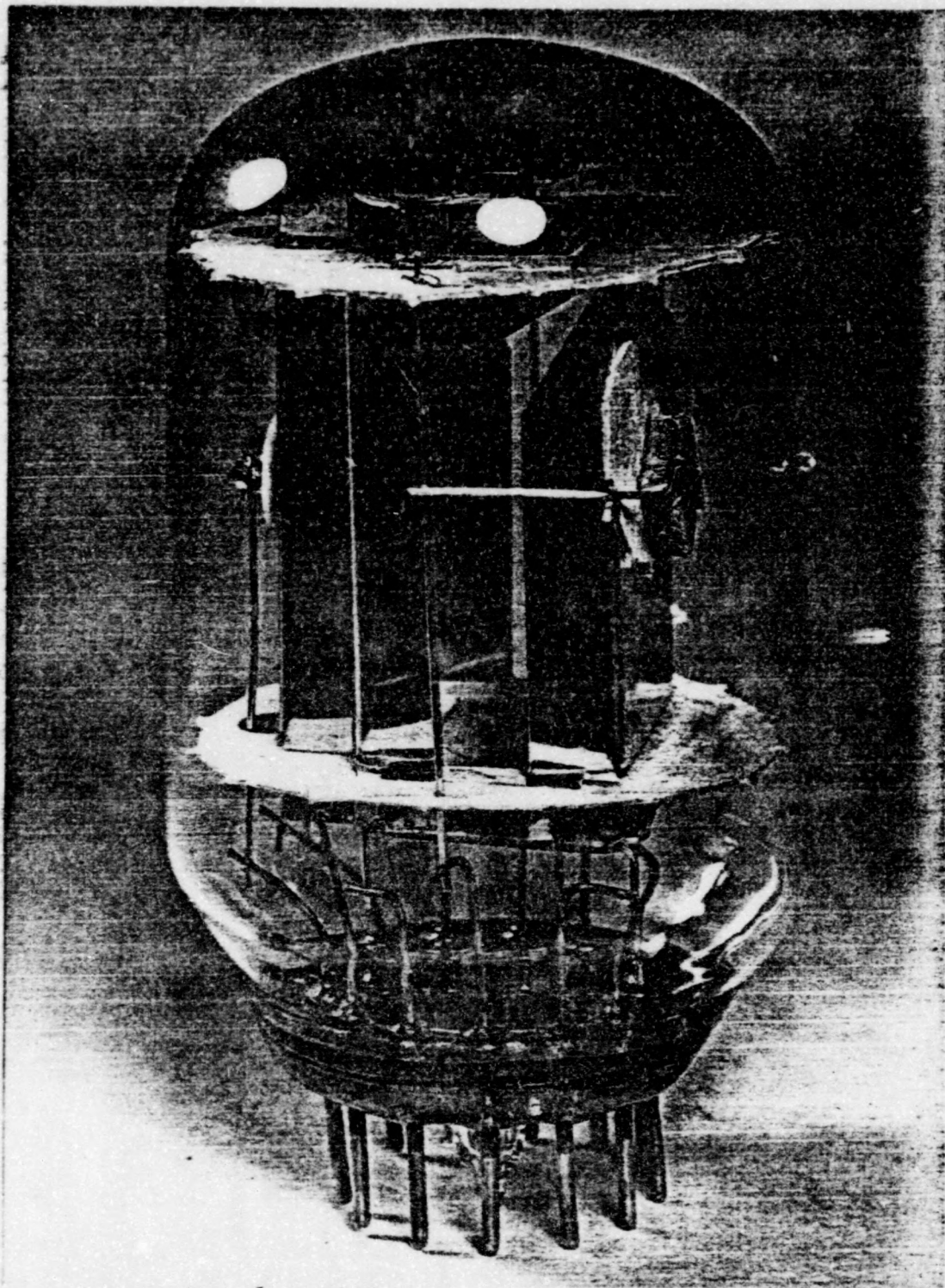


Figure 9. Zero electric field device.

CHAPTER III

EXPERIMENTAL RESULTS

During evaluation of the initial pencil beam device it was discovered that the electron gun was being cut off because of the application of the magnetic field developed by the Helmholtz coil. This can be seen in Figure 11. The current to the second accelerator electrode inside the Pierce gun increased markedly when the strength of the magnetic field was increased indicating the electron beam inside the gun was deflected. Various shapes, thicknesses, numbers and orders of layers of Mu metal, Netic and Conetic material were evaluated to find a satisfactory magnetic shielding for the gun. The results of this investigation are shown in Figures 11 and 12. One layer of Netic material on the outside of two layers of Conetic material provides sufficient shielding when the magnetic field range is between 0 and 35 gauss. A cylinder of Mu metal 1/16" thick was also found to provide similarly satisfactory shielding. Addition of the shielding caused perturbation of the magnetic field between the plates of the trochoidal device.

Measurements indicated that the disturbance of the magnetic field would be reduced to an acceptable level if the shielded gun could be

moved 1 cm or more away from the bottom electrode. This separation would necessitate projecting the electrons through a cylinder made of suitable shielding material with a very small diameter. A 10% change in the field near the end of a .030" x 20 mm cylindrical nickel cathode sleeve was measured when it was mounted with its longitudinal axis perpendicular to a field of 1.5 gauss. It can be seen from the photographs of the devices that there was not room to move the electron source away from the bottom electrode and use the same bulb.

Three other methods of shielding were considered. One idea was to put a set of miniature Helmholtz coils around the electron source to cancel the external magnetic field. Also studied was the possibility of enclosing the gun inside a tightly wound toroid with ejected electrons emerging from between two slightly displaced turns. Measurements made with a gauss meter indicated that with a 10 gauss field inside an experimental coil, the external field could be reduced to .1 gauss. Brief consideration was given to the use of electrostatic deflection plates oriented in such a manner as to cancel the magnetic force. Space limitations caused the three ideas to be dropped.

All of the devices were evaluated in essentially the same manner. An electron beam of known energy level was generated. Then the magnetic field was varied with electrical potentials on the electrodes and collector. Peaks of collector current which represented the beam current with no bounce and one bounce were recorded. Because of beam

spreading the peaks were not sharply defined and an accurate value of reflection coefficient could not be determined. K. E. Garrison, research assistant at Western Kentucky University, devised a method whereby the peaks of collector current were broken up into parts so that each section corresponded to the current that would go through one slit width if the beam were held stationary. This method is summarized below:

1. The derivative of the standard range equation for an electron in a trochoidal path was taken with respect to the magnetic field (B).
2. Values within the desired range of the magnetic field were inserted into the equation and a curve of dx/dB versus B was plotted (Figure 10) so that approximate values of dx/dB could be determined between the points actually inserted into the equation.
3. The change in the magnetic field corresponding to 1 slit width was determined by the equation $\Delta x = (dx/dB)\Delta B$ where Δx was one millimeter and dx/dB was an average value. The value of dx/dB was determined by averaging the endpoint values

$$\frac{\frac{dx}{dB}(B) + \frac{dx}{dB}(B + \Delta B)}{2}$$

4. The value of current at the midpoint of each section was determined.
5. The midpoint current values in each curve were added separately.
6. The ratio of the two sums gave a value of reflection coefficient.

When the above method was used to evaluate data taken on the sheet beam device values of reflection coefficient were calculated which ranged between 4% and 12%.

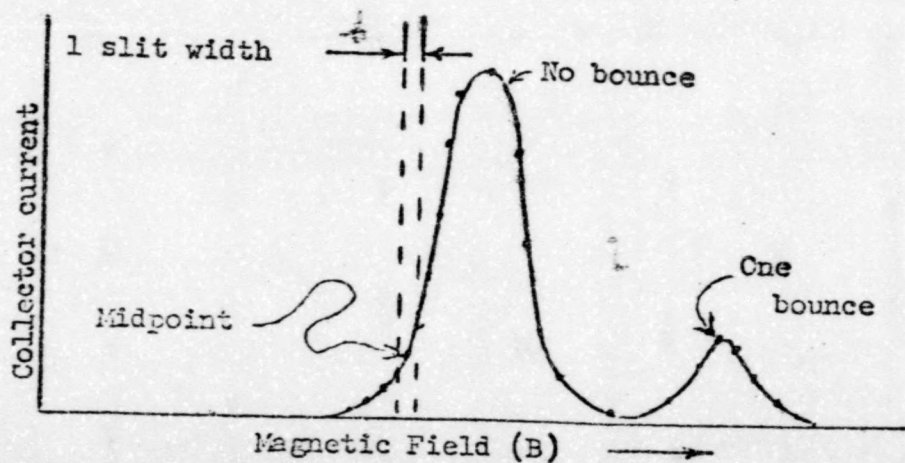
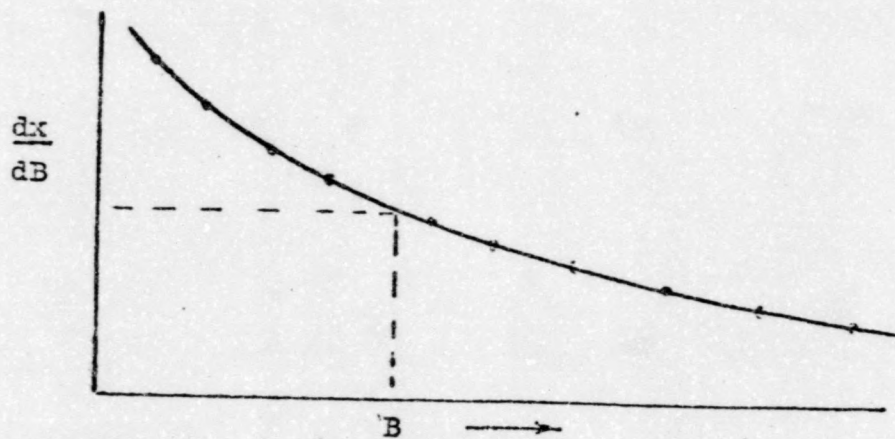
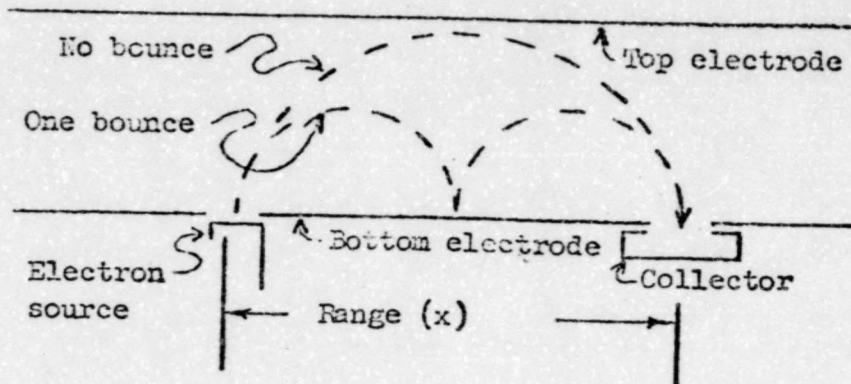


Figure 10. Diagram of apparatus and curves showing method used to find reflection coefficient.

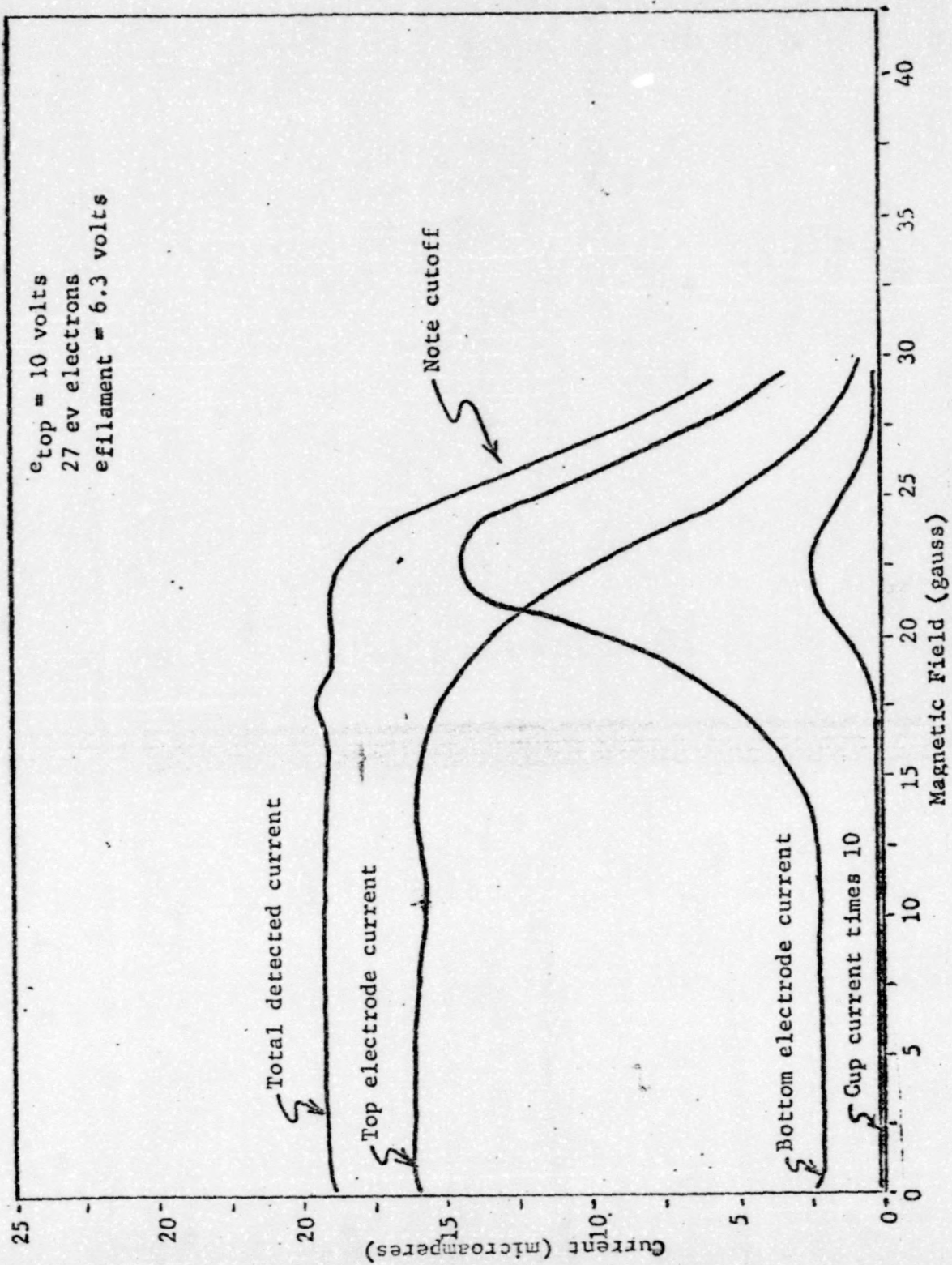


Figure 11. Data taken during operation of initial pencil beam device.

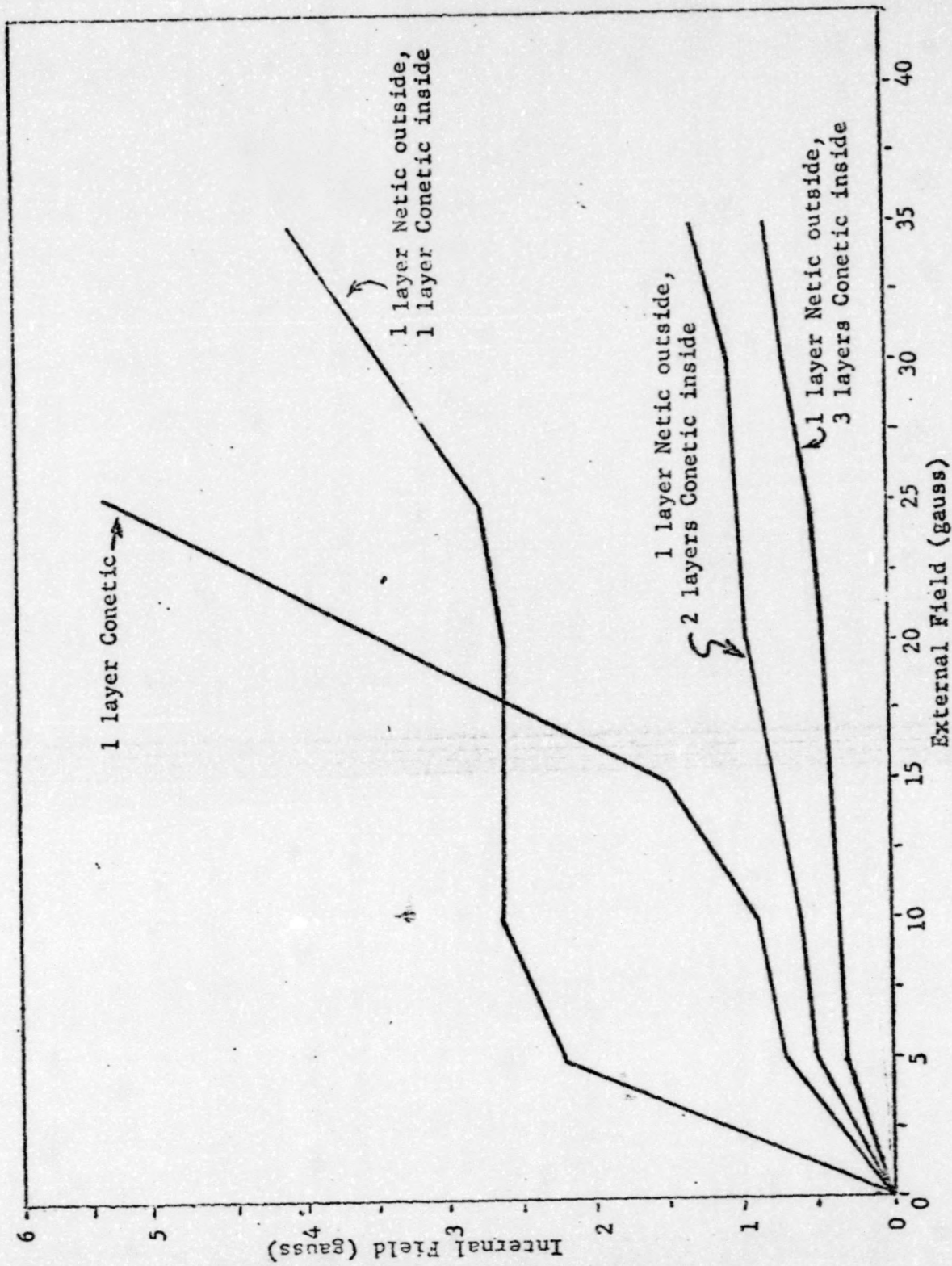
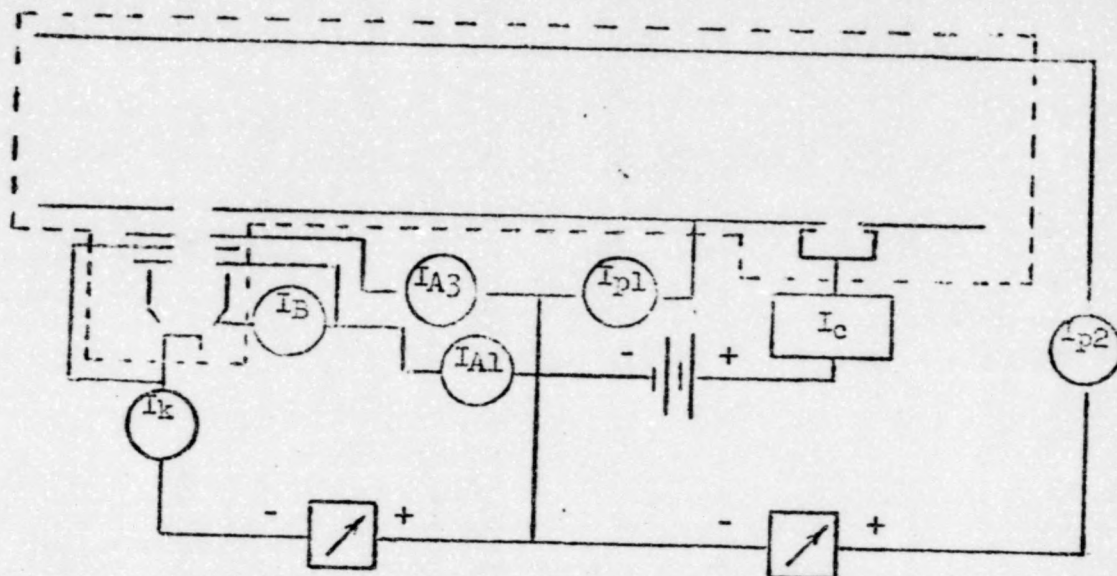


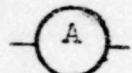
Figure 12. Investigation of magnetic shielding materials.



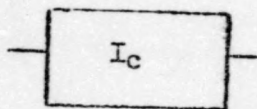
Heathkit Transistorized Power Supply,
0 to 35 volts, 0 to .5 amperes



Galvanometers of various sensitivities,
(I_{A3} , I_{p1} , I_{p2} , I_c)



Milliammeters of various sensitivities,
(I_k , I_B and I_{A1})



Keithley Electrometer, Model 610 A used to
measure I_c

Figure 13. Circuit used to evaluate final pencil beam device.

TABLE I

Data taken from pencil beam final device

Ex. Field (Gauss)	I_2	I_A	I_B	I_{A1}	I_{A3}	I_{p1}	I_{p2}
5	4	0.49 ma	0.33 ma	0.36	0	0	0.1 μ a
5	5	0.49 μ a	.33	.36	1 μ a	0	0.1 μ a
10	5	1.37 ma	.92	1.07	3.5 μ a	1 μ a	0.45 μ a
	20	no change	--	--	--	--	--
12.5	5	1.79 ma	1.195	1.38	4.5 μ a	1 μ a	0.70 μ a
	10						0.75 μ a
	20						0.82 μ a
15	5	2.22 ma	1.57 ma	1.78 ma	6.2 μ a	1.5 μ a	1.0 μ a
	10						1.05
	15						1.1
	20						1.15
17.5	5	2.68 ma	1.8 ma	2.17 ma	7.5 μ a	2 μ a	1.3 μ a
	10						1.4
	15						1.5
	20						1.55
20	5	3.21 ma	2.32 ma	2.62 ma	9.5 μ a	2+ μ a	1.75 μ a
	10						1.9
	15						2.0
	20						2.05
22.5	5	3.85 ma	2.74 ma	3.05 ma	11.0 μ a	2.5 μ a	2.25 μ a
	10					2.5 μ a	2.45
	15				10.8	2.5	2.55
	20						2.6
25	5	4.35 ma	3.13 ma	3.55 ma	13 μ a	3 μ a	2.8 a
	10					2.5 +	3.1
	15					2.5 +	3.25
	20					2.5 +	3.3
27.5	5	4.85	3.48 ma	3.95 ma	14.5 ma	3 μ a	3.4
	10					2.5 +	3.7
	15					2.5 +	3.85
	20					2.5	3.9
30	5	5.3 ma	3.92 ma	4.42 ma	16.0 μ a	3.0 μ a	3.9 μ a
	10					2.5 +	4.25
	15					2.5 +	4.45
	20					2.5 +	4.55
40	5	7.1 ma	5.42 ma	6.05 ma	25 μ a	4.0 + μ a	6.6 μ a
	10				25 +	4.0	7.25 μ a
	15				25.5	3.5 +	8.65
	20				25.5	3.5	8.65
50	5	9.0 ma	6.8 ma	7.85 ma	35.5 μ a	5.5 μ a	9.95 μ a
	10				35.5 +	4.5 μ a	11.0
	15				36	4.5	11.45
	20				36 +	4.5 -	11.75
	25				36 +	4.5 -	11.9
60	5	10.5 ma	7.95 ma	9.45 ma	47.5 μ a	6.5 μ a	13.25
	10				48	6.5	14.7
	15				50 water change	6.0	14.0 water change
	20	11.0	8.15 ma	9.65 ma	52	6.0	14.5
	25				52	5.5 +	15.5
	30				52	5.5	15.8
70	5	13.0	9.35	11.7	75	9.0	18.8
	10					6.0 +	20
	15					5.5	21
	20				73	5.0	21 +
	25					5.0	21

NOTE: $E_f = 6.1$ volts at 279 ma

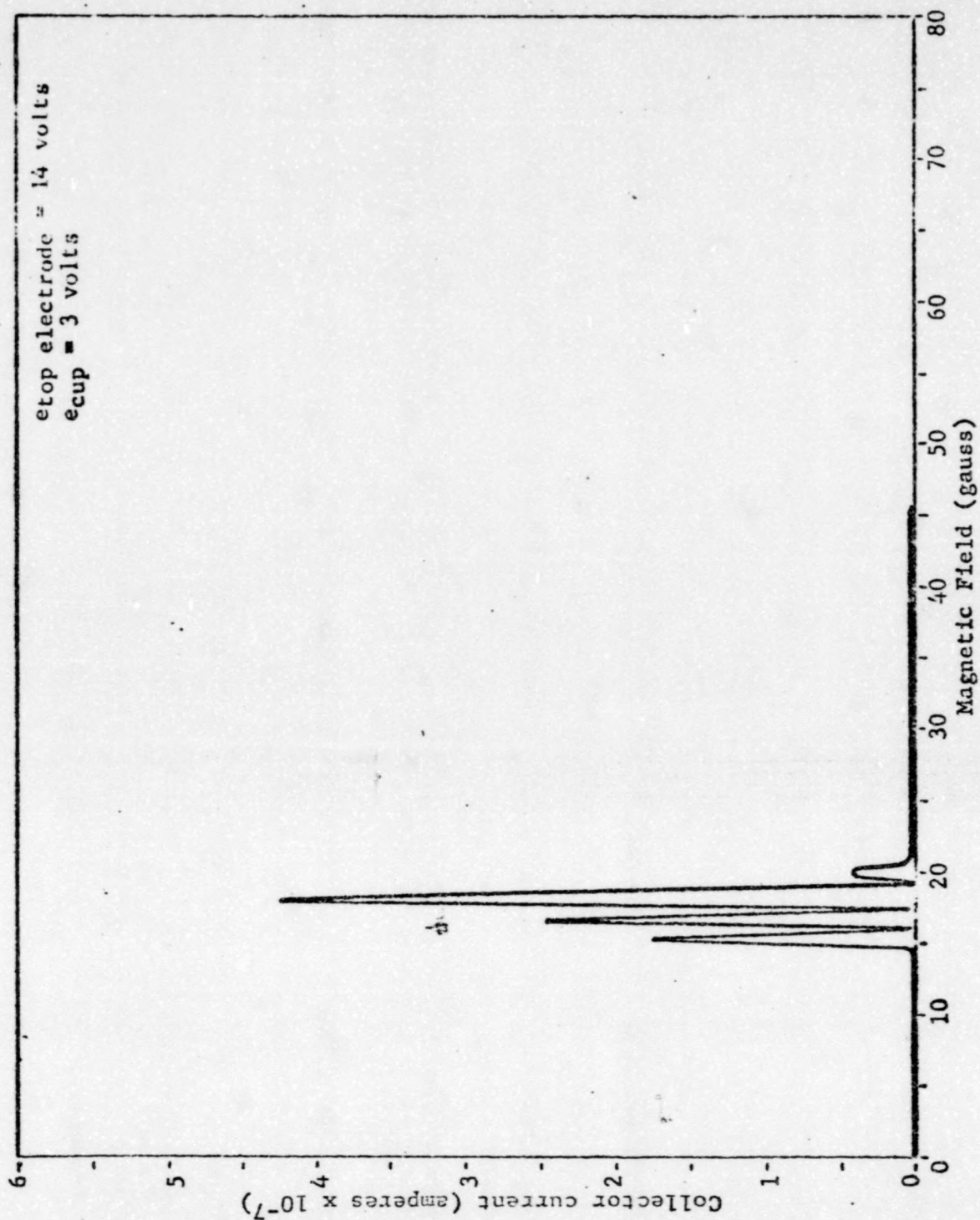


Figure 14. Final pencil beam device collector current versus magnetic field for 2 ev electrons.

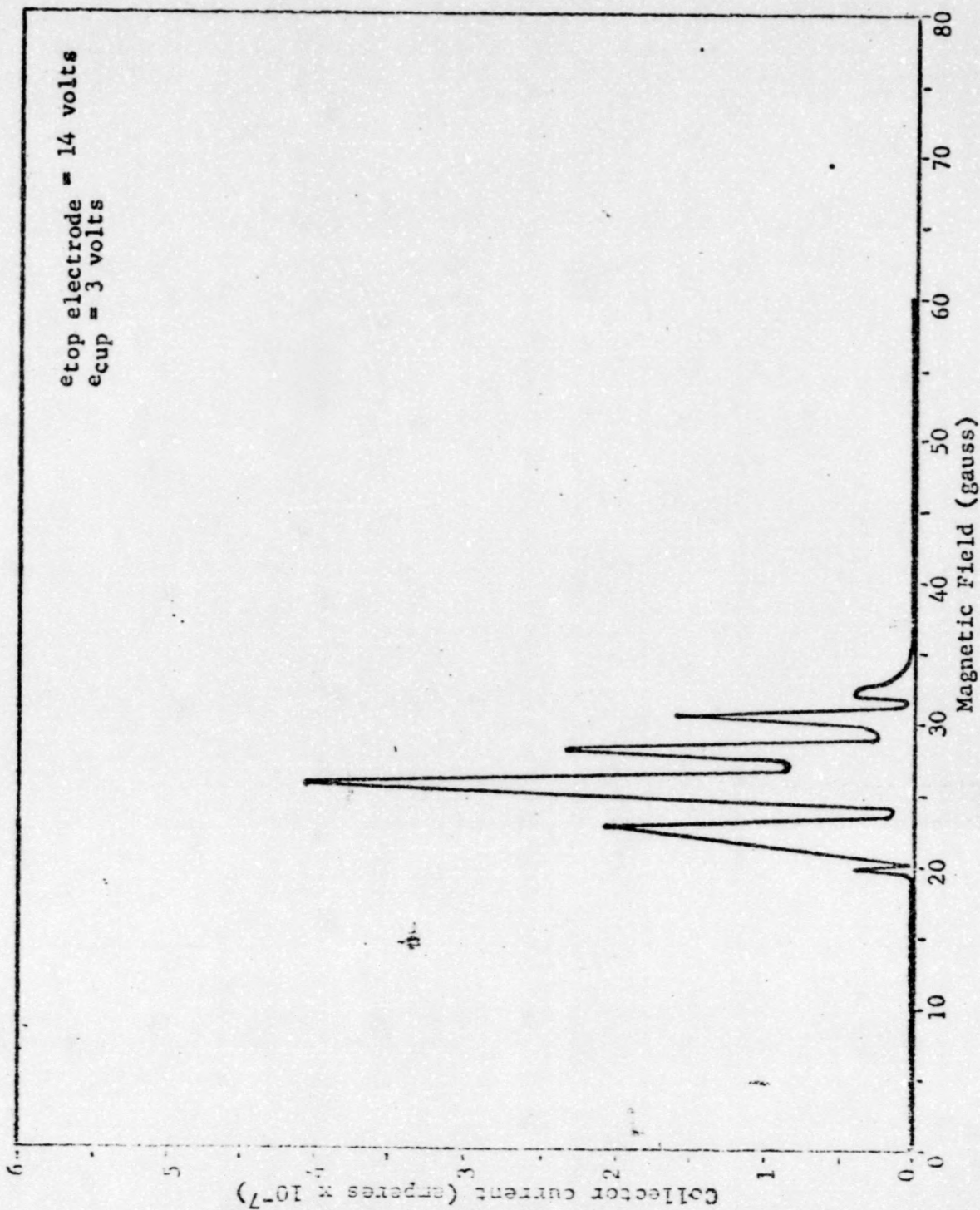


Figure 15. Final pencil beam device collector current versus magnetic field for 4 eV electrons.

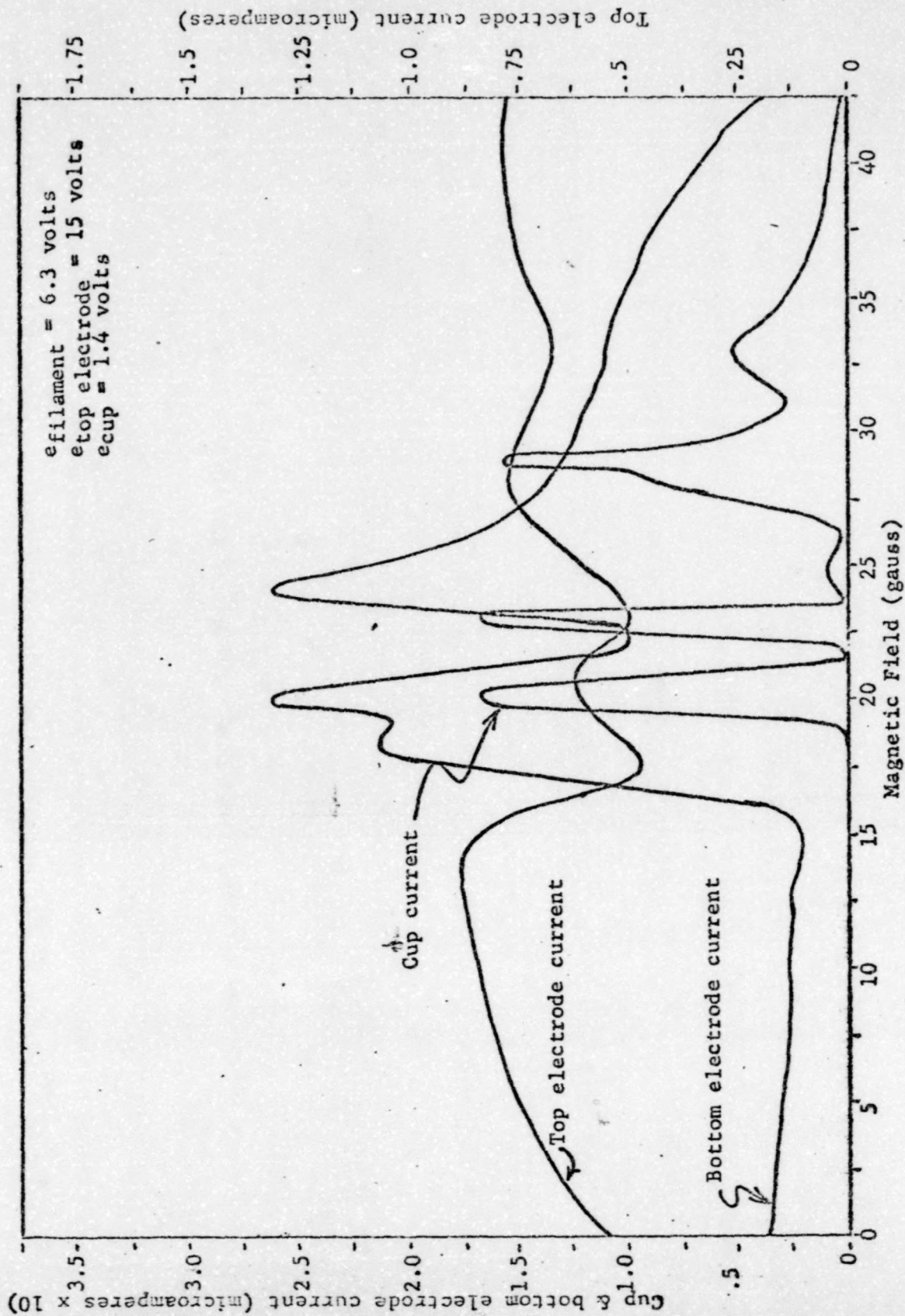
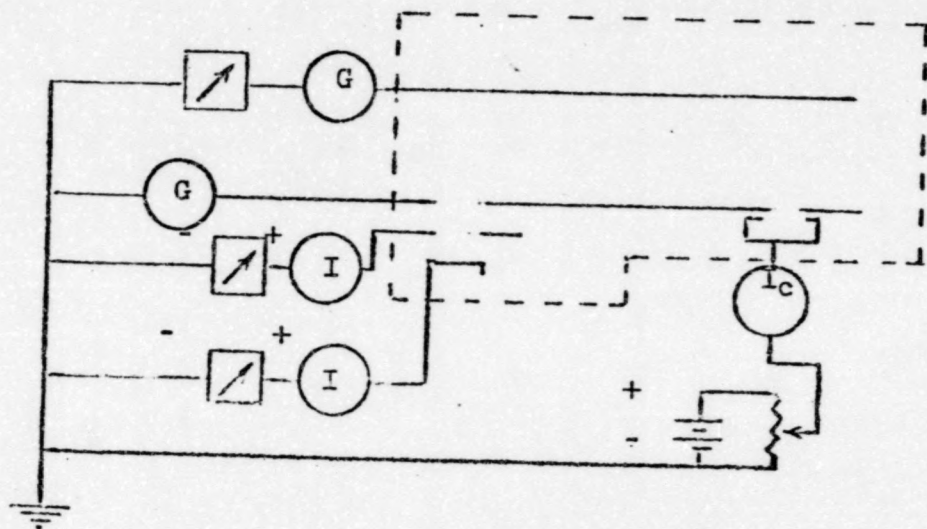


Figure 16. Data taken during operation of pencil beam device for 5 ev electrons.






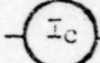
- 
 Heathkit Transistorized Power Supply,
 0 to 35 Volts, 0 to .5 Amperes
- 
 Galvanometers of various sensitivities
- 
 Milliampmeters of various sensitivities
- 
 Keithley Electrometer, Model 610 A

Figure 17. Circuit used to evaluate sheet beam device.

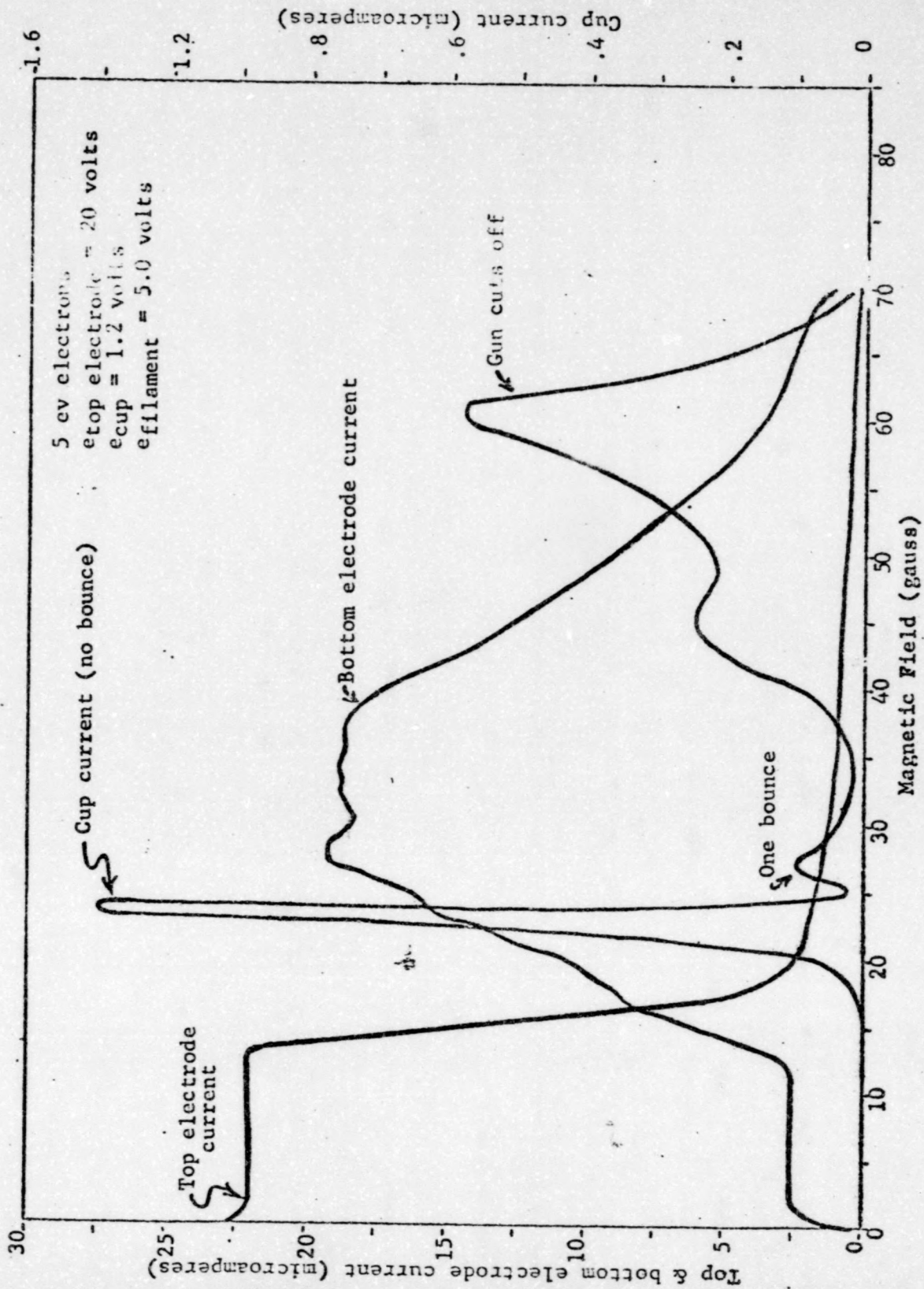


Figure 18. Sheet beam device cup & electrode current versus magnetic field for 5 ev electrons.

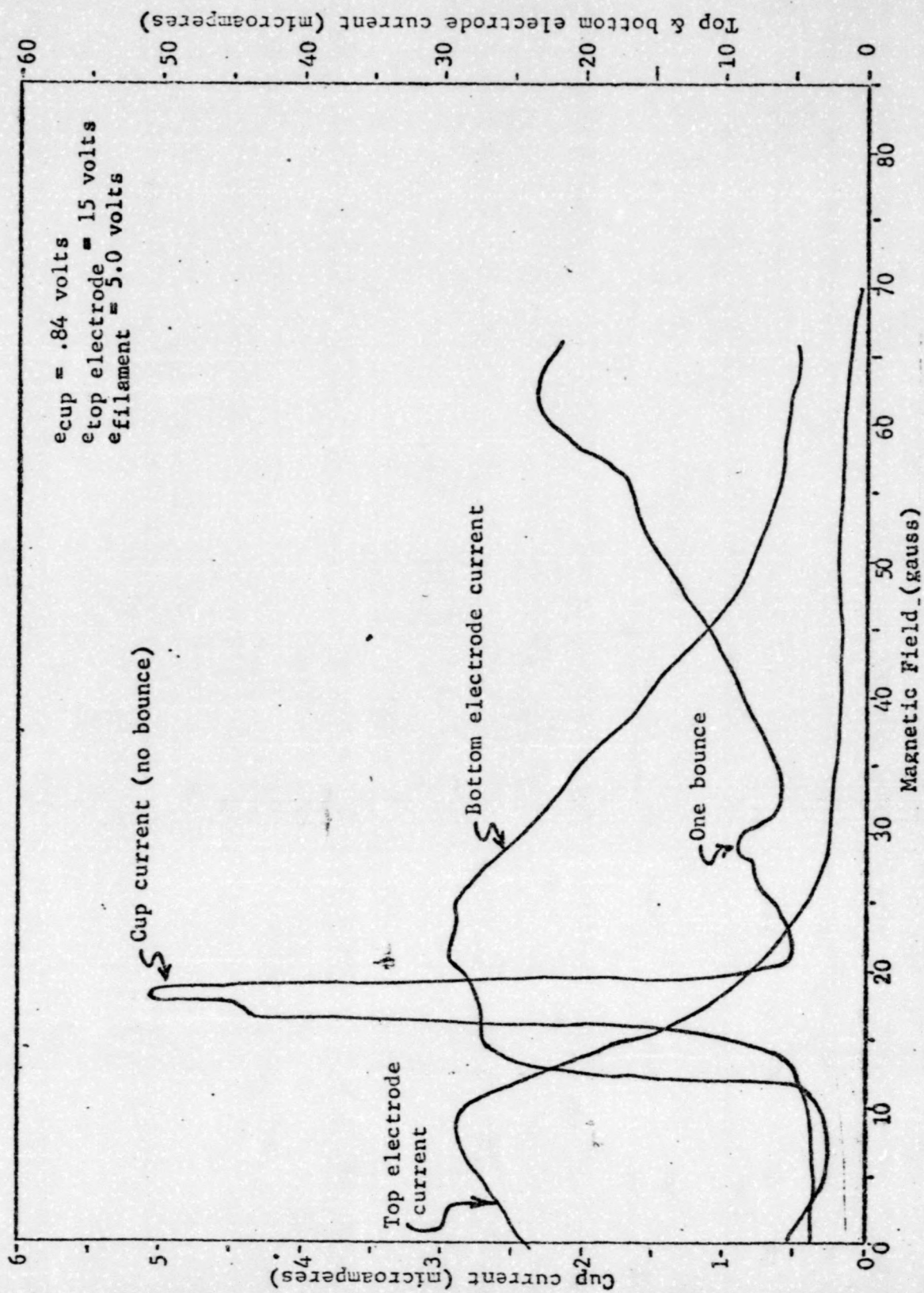


Figure 19. Sheet beam device cup & electrode current versus magnetic field for 10 ev electrons.

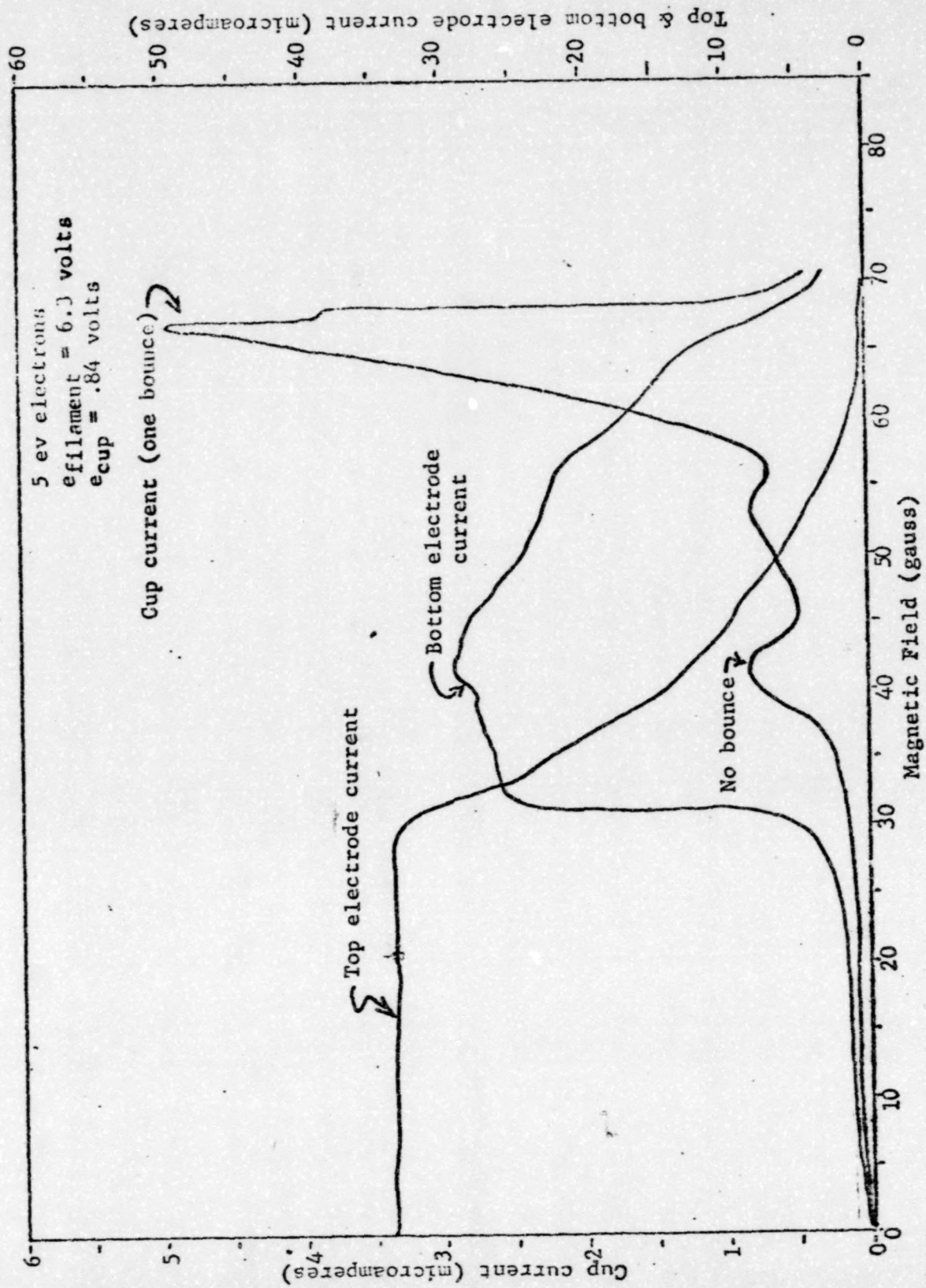


Figure 20. Sheet beam device cup current versus magnetic field for 91 volt top electrode potential.

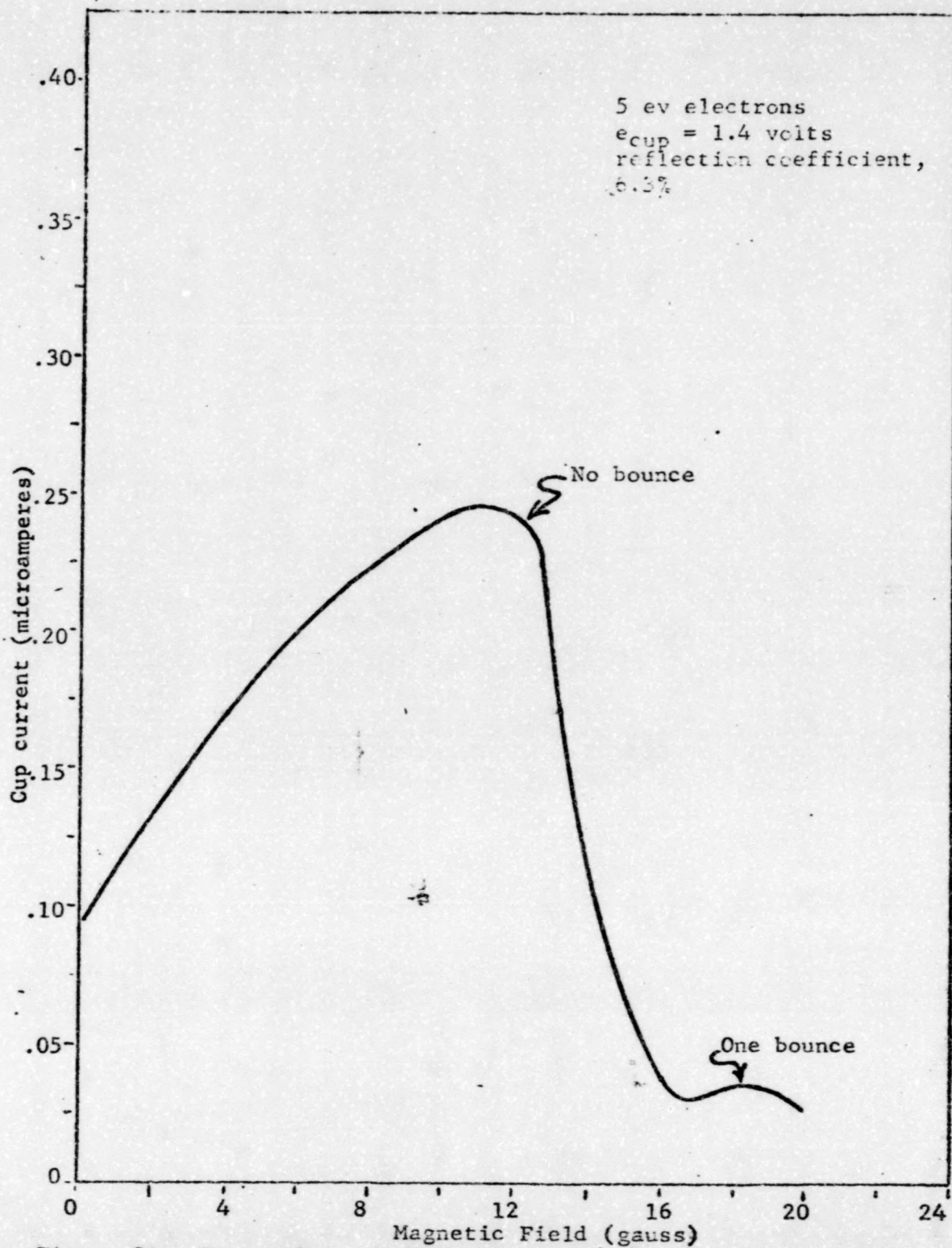
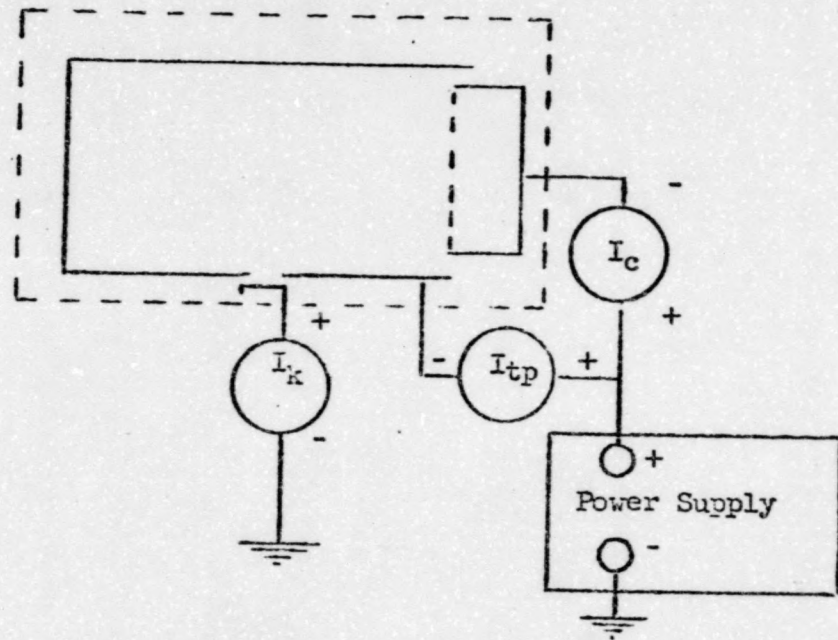


Figure 21. Data taken on sheet beam device to determine reflection coefficient.




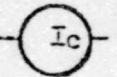

-  Cathode current
-  Cup current
-  Top electrode current

Figure 22. Circuit used to evaluate zero electric field device.

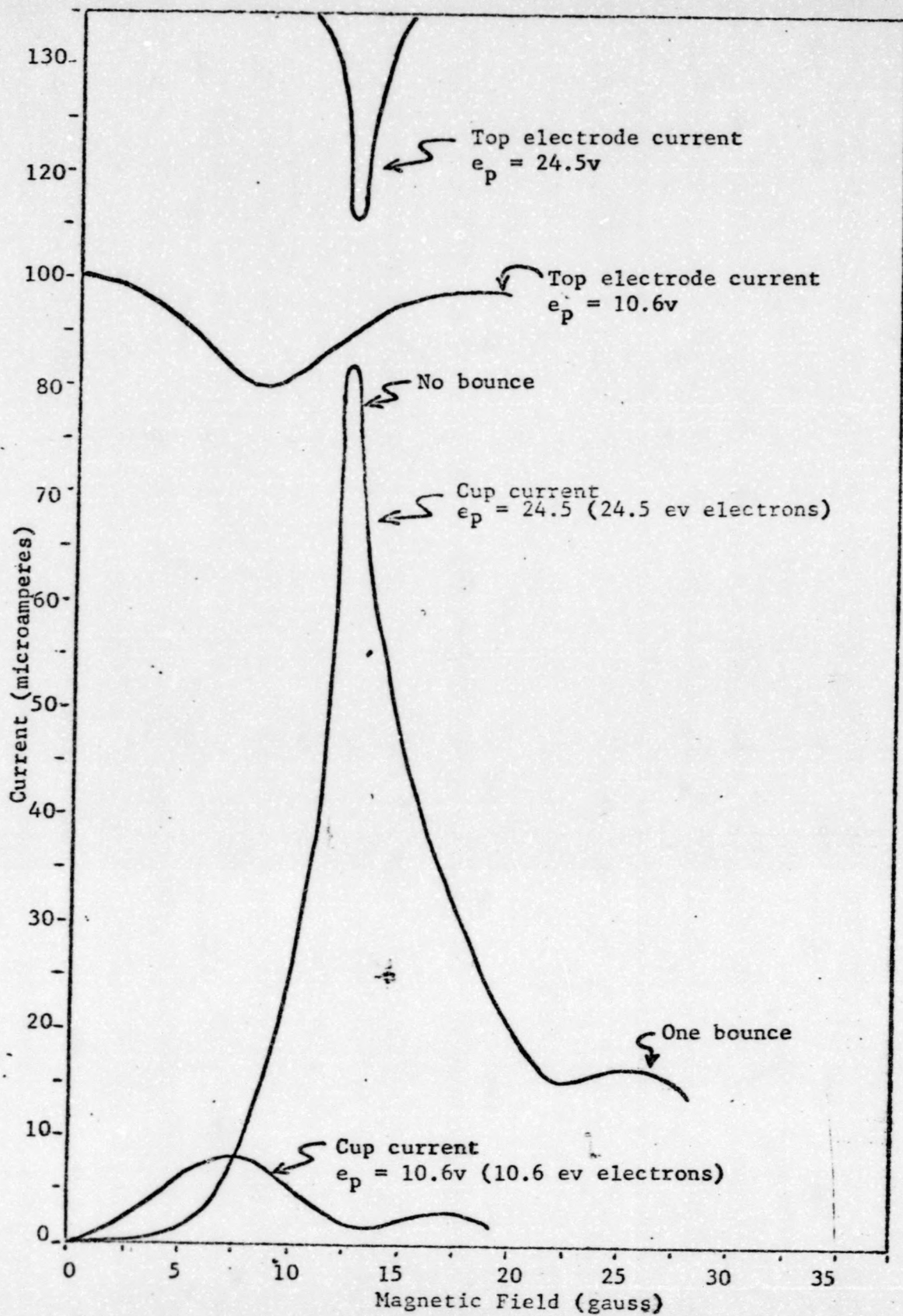


Figure 23. Cup & top electrode current vs. magnetic field for zero electric field device.

TABLE II

Data taken from zero electric field device.

$E_{\text{top Plate}}$ (Volts)	I_{cup} (Microamperes) <u>Maximum</u>	$I_{\text{top Plate}}$ (Microamperes) <u>Minimum</u>	I_f (Amperes)	Field Strength (Gauss)
10	86	13	1.8	7.2
15	103	61	2.5	10.0
20	116	68	3.0	12.0
25	128	87	3.5	14.0
30	137	140	3.8	15.2
35	146	155	4.3	17.2

CHAPTER IV

ANALYSIS OF RESULTS

One difficulty encountered in the sheet beam device was that when the beam was bent sufficiently to cause the collector to draw current the top plate current did not go to zero as anticipated. A model of the sheet beam device was built with mercury inside. The ionization of the mercury gas (Figure 24) clearly showed the beam spreading out to an angle of approximately 56 degrees. When the magnetic field was applied, the wedge shaped beam leaned over in the direction predicted by theory. However, at no time did the beam bend at such an angle that the trailing edge of the beam did not touch the top plate. A strange phenomenon was observed to occur when the collector current was initiated. A tiny streak was seen inside the gas. The small stream bent in the arc expected and its radius could be increased or decreased by changing the magnitude of the applied field.

The final pencil beam device which was designed to cause the electron beam to go through two bounces before being intercepted by the collector failed to produce more than one peak of collector current. Since reflection coefficient is the ratio of two values of current it could not be calculated. In the single peak (Figures 14, 15 and 16) of

collector current diffraction effects can be noted. The diffraction effects occurred when the beam grazed the top electrode.

The sheet beam device was successful in producing multiple peaks of collector current which permitted reflection coefficient values to be calculated. The peaks were wider than had been anticipated which caused the calculated values of reflection coefficient to be questionable. The broadness of the peaks was due primarily to beam spreading. It will be noted in Figures 18, 19 and 20 that when the top electrode potential is increased from 20 to 91 volts the device is no longer useful for obtaining suitable peaks.

The zero field device produced peaks (Figure 23) from which values of reflection coefficients could be measured, but the widths of the peaks were excessive.

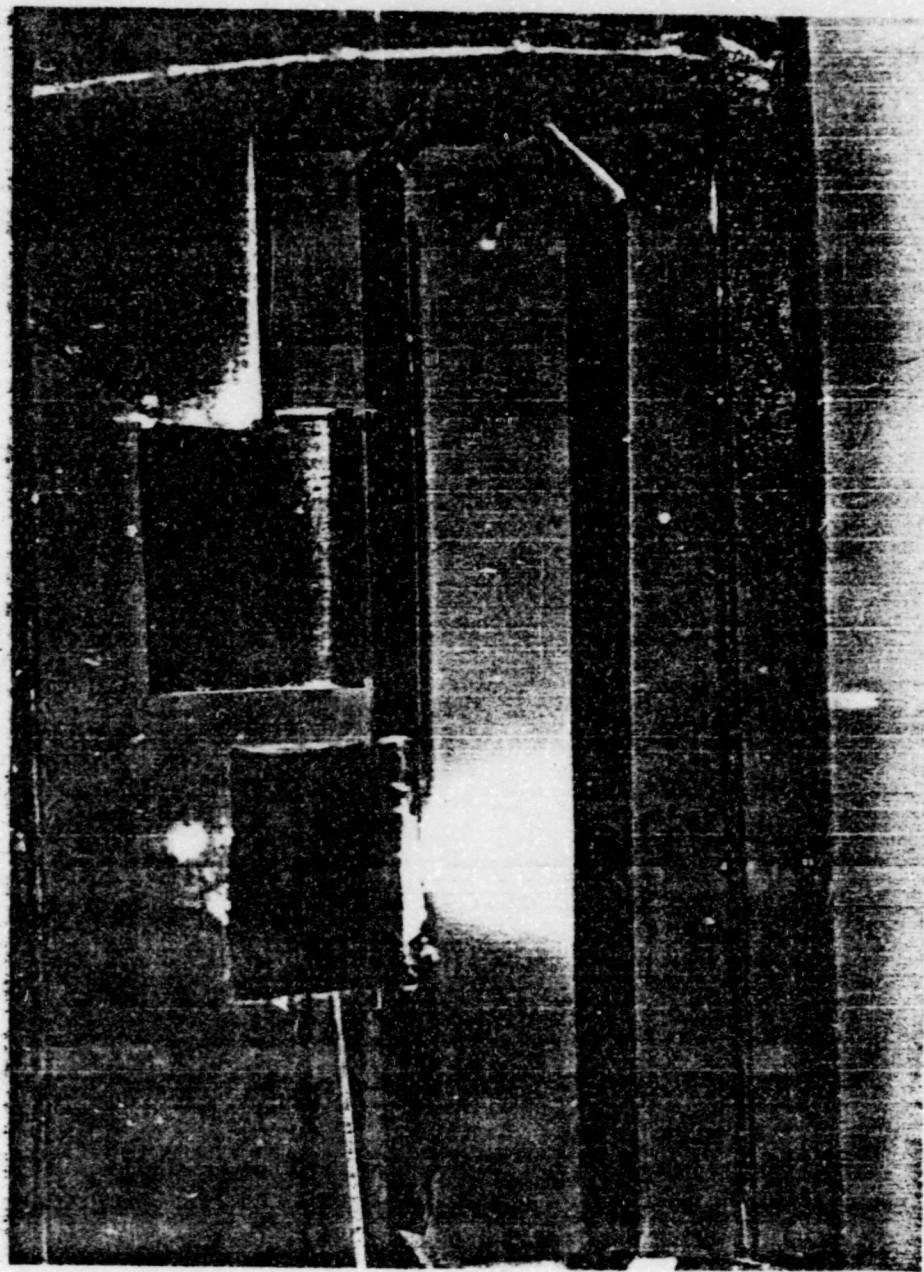


Figure 24. Sheet beam device with ionized mercury gas inside.

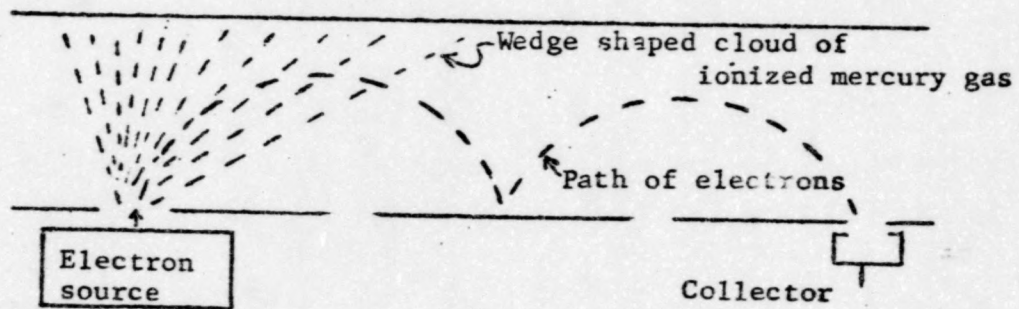


Figure 25. Ionization patterns observed inside the sheet beam device during operation with mercury gas inside.

COMPARISON OF THE VARIOUS TROCHOIDAL DEVICES

Since none of the devices built yielded satisfactory data from which to calculate reflection coefficients they cannot be compared on that basis.

Usefulness as a tool for measuring reflection coefficients.

Initial pencil beam device - not satisfactory because the externally applied magnetic field cut the electron gun off before peaks of cup current could be established.

Final pencil beam device - not satisfactory because of beam spreading and the inability to generate a monochromatic electron beam. Beam spreading was worse with this design and so severe that results were difficult to interpret.

Sheet beam device - not satisfactory because of beam spreading and lack of monochromatic energy in electron stream from its gun. This device produced peaks of cup current and crude values of reflection coefficients were calculated.

Zero electric field device - although not satisfactory because of beam spreading this device is more practical than the others because of its simpler design.

SUMMARY

Beam spreading was an extreme problem in all devices. Beam spreading became worse when the current density of the electron beam was increased and/or when the electron velocity was reduced. Because of the spreading of the beam the collector was too small in cross-sectional area to intercept all of the reflected electrons thus making the subsequent calculations of reflection coefficient subject to doubt. Diffraction effects were observed in the collector current measurements when circuit conditions were such that the electron beam grazed the top electrode. No electron gun designs tried during this study were capable of providing a monochromatic electron beam. The beam of electrons generated by the electron guns were severely affected by the application of the external magnetic field. The external magnetic field bent the beam while it was still inside the gun thus preventing the electrons from making normal entry into the electric field. Shielding the electron guns from the external magnetic field introduced distortion of the field.

RECOMMENDATIONS FOR FUTURE WORK

Any future devices should be designed to minimize beam spreading but should not be built until an electron source is available which can supply monochromatic electrons. This will require that a velocity selector must be an integral part of the electron gun. The magnitude of the electron beam current should be at the lowest possible value that results in satisfactory data and the collector must have a cross-sectional area large enough to intercept all of the reflected electrons. It would be helpful if the collector were divided into several sections so that a better idea of the width of the beam might be determined. It is more practical to mount the devices inside a bell jar vacuum system instead of inside a sealed glass envelope because mechanical changes can be made easily by removing the bell jar whereas the sealed device is a one shot study. Useful information concerning a device may be obtained by putting a substance capable of fluorescing on the areas of the electrodes and collector which will be struck by the impinging electrons. This technique permits a visual observation of beam spreading. Also the devices can be filled with a gas capable of being ionized under the conditions used in the experiment. With a bell jar vacuum system, the bell jar itself could be used as a collector by putting a conductive coating on its inner surface.

LIST OF REFERENCES

1. Russell, M. W. An Investigation of Slow Electrons from Surfaces. Quarterly Status Reports I, II, III,, Report #1, June 1, 1966 - August 31, 1966.
2. Harrower, G. A. Energy Spectra of Secondary Electrons from Mo and W for Low Primary Energies, Physical Review, Volume 104, Number 1, October 1, 1956, pp. 56-56.
3. Kohl, W. H. Handbook of Materials and Techniques for Vacuum Devices. New York: Reinhold Publishing Corporation, 1967.
4. Goble, A. T. and Baker D. K. Elements of Modern Physics. New York: Ronald Press Company, 1962, p. 138.
5. Goble, op. cit., p. 46.
6. Russell, op. cit., Report 1.

BIOGRAPHICAL SKETCH

S. W. Lemaster, Design Engineer, General Electric Company.

Mr. Lemaster received his B. S. Degree in Electrical Engineering from Oklahoma State University in 1951. From graduation to the present date he has been employed as a Design Engineer by the General Electric Company. During this time he designed new receiving tube types, investigated tube materials and processes to improve manufacture. He has authored seven internal papers of a proprietary nature and holds two patents (#3,263,299 and #3,238,405).

Mr. Lemaster has taught fifteen night courses: Brescia College (Physics) 8 semesters, Kentucky Wesleyan College (Physics, Algebra and Trigonometry) 4 semesters, and Owensboro Area Vocational School (Radio, Electronics and Transistor Theory) 3 semesters.

Mr. Lemaster is Past Chairman of the Evansville-Owensboro section of IEEE.